Nanochem Res 8(3): 215-223 Summer 2023

RESEARCH PAPER

A facile one-step electrochemical preparation of graphene–Pd nanocomposite as a catalyst for hydrogen evolution reaction

Fatemeh Norouz-Sarvestani[1], Seyyed Mehdi Khoshfetrat[*2]

[1]Department of Chemistry, College of Sciences, Shiraz University, Shiraz, Iran
[2]Department of Chemistry, Faculty of Basic Science, Ayatollah Boroujerdi University, Boroujerd, Iran

ARTICLE INFO

Article History:
Received 09 Mar 2023
Accepted 21 May 2023
Published 27 May 2023

Keywords:
Electrodeposition
Graphene
PdNPs
Hydrogen evolution reaction
CPE

ABSTRACT

This study describes a one-step, facile, simple, and effective electrochemical method for the codeposition of graphene oxide (GO) and Pd nanoparticles (NPs) onto a carbon paste electrode (CPE). The obtained nanocomposite was characterized using scanning electron microscopy, cyclic voltammetry, and chronocoulometry techniques, which confirmed the high dispersion and stability of PdNPs supported on the graphene. This procedure does not require the use of a reducing agent or surfactant, making the preparation process very clean. This catalyst showed superior electrocatalytic activity and stability toward hydrogen evolution reaction (HER) when compared to either PdNPs or graphene alone, indicating the synergistic effect of graphene and PdNPs. The Tafel slopes of HER on both bare and modified CPE were determined to be 97 and 146 mV dec^{-1}, respectively. In addition, the kinetic parameters showed that the Volmer step must control the HER. This study suggests an effective and controllable method for preparing graphene–metal NPs with high electrocatalytic activity.

How to cite this article
Norouz-Sarvestani F., Khoshfetrat S. M., A facile one-step electrochemical preparation of graphene–Pd nanocomposite as a catalyst for hydrogen evolution reaction. Nanochem Res, 2023; 8(3): 215-223 DOI: 10.22036/ncr.2023.03.007

INTRODUCTION

Hydrogen is considered a promising source of green energy owing to its high energy density, environmental friendliness, safety, and cleanliness [1, 2]. To facilitate the production of hydrogen, cathode electrode materials with favorable properties such as high electrocatalytic activity (to reduce overpotential), a sizable active surface area, moderate electrochemical stability, strong electrical conductivity, and ease of use are required [3]. Although Pt or Pt based catalysts are effective HER catalysts, their high cost and scarcity limit their widespread application [4]. On the other hand, Pd metal can serve as a good substitute for Pt due to its relative abundance in the Earth's crust and lower price [5]. Graphene, a two-dimensional honeycomb lattice of carbon atoms, is a fundamental structural component of several carbon allotropes, such as graphite, carbon nanotubes, and fullerenes [6]. Due to its large surface area, aspect ratio, tensile strength, thermal and electrical conductivity, flexibility, and transparency, graphene is also regarded as the best carbon nanofiller when compared to other traditional nanofillers [7, 8].

Metal nanoparticles can be supported by using graphene or reduced graphene oxide (rGO). Due to their size-dependent properties, metal NPs are of tremendous scientific interest, and their efficacy in catalysis can be improved by carefully regulating their size and shape [9-11]. During the synthesis of metal nanoparticles (MNPs), the uncontrolled development and agglomeration of large particles can result in the loss of their dispersibility and other beneficial features [12]. Therefore, the synthesis of MNPs with controllable size, homogeneous morphology, good crystallinity, and high

* Corresponding Author Email: m.khoshfetrat@gmail.com

This work is licensed under the Creative Commons Attribution 4.0 International License.
To view a copy of this license, visit http://creativecommons.org/licenses/by/4.0/.

dispersion is crucial. Reduced graphene oxide (rGO) is expected to be the best catalyst carrier for this purpose because it provides a good 2D support for nucleating and anchoring metal NPs on the edges and surface [13-15]. Due to its crinkly structure and the oxygen atoms, it managed to hold onto its film and decrease NP aggregation. Electrodeposition is the most reliable and controllable technology for the synthesis of metal NPs due to its straightforward process, capacity to regulate the size and shape of the nanoparticles, and its relatively short completion time [16-18]. GO can be reduced through both chemical and electrochemical processes. Chemical reducing agents, such as hydrazine hydrate [19], sodium borohydride [20], nascent hydrogen [21], sulfur-containing compounds [22], and ascorbic acid [23], are frequently used in the production of graphene. However, the use of reducing agents poses several drawbacks such as prolonged thermal process for the deoxygenation, toxicity of the chemical reductants, and extremely harsh reaction conditions. Furthermore, such agents may adversely impact the fundamental properties of graphene and result in time-consuming and complicated processes. Moreover, some epoxide groups on GO cannot be entirely reduced using these procedures, which would diminish the effectiveness of electron transport and weaken the electrochemical activity. Therefore, electrochemical procedures have been carried out without the use of any reducing chemicals. These methods have recently gained significant attention because of their quick, environmentally friendly, controlled, strong, and effective way of removing oxygenation fault spots from GO and enhancing their electrical characteristics.

In this study, a one-step and simple electrochemical technique was employed to prepare rGO and PdNPs on CPE. The resulting nanocomposites (Pd-rGO) were analyzed using scanning electron microscopy (SEM), cyclic voltammetry (CV), and chronocoulometry (CC) techniques. The density and morphology of PdNPs on the surface of graphene appear to be markedly different from those that were simply deposited on the bare CPE surface (Pd/CPE). Moreover, the created Pd-rGO nanocomposites exhibit an effective electrocatalytic activity on HER. Along with having high electrocatalytic activity, Pd-rGO is also more stable in acidic environments than Pd/CPE. This is caused by the interpenetrating network that rGO creates to immobilize PdNPs.

EXPERIMENTAL

Reagents and apparatus

A modified Hummer's process was used for making the graphene oxide (GO), and $PdCl_2$ was extracted from Fluka. All other compounds were used without purification since they were all of analytical grade. Deionized water was used to make all stock and buffer solutions, and experiments were conducted at room temperature. An Autolab type III was employed to carry out electrodeposition, CV, and CC, utilizing GPES version 4.9 operating system. In this investigation, a three-electrode setup was employed, consisting of an Ag|AgCl| 3 M KCl reference electrode, a Pt wire as a counter electrode, and a bare or modified CPE as the working electrode. A Teflon cylinder (with a 2.0 mm inside diameter) filled with carbon paste served as the body of the working electrode, and electrical contact was established by inserting a stainless steel rod into the Teflon tube containing the carbon paste. The morphology of the nanoparticle-modified electrodes was analyzed using a Leica Cambridge model S 360 SEM with a 25 keV accelerating voltage. Ultra-pure N_2 was utilized to deaerate the solutions for at least 15 min before each run, and all tests were conducted under a N_2 atmosphere after degassing the solutions.

Electrode preparation

After preparing the carbon paste by combining graphite powder and paraffin oil (70:30 w/w), a portion of it was firmly packed into the cavity (with a 2.0 mm diameter) of a Teflon tube. To establish electrical connection, a stainless steel rod was inserted into the tube containing the carbon paste. Polishing paper was used to polish and smooth the surface of the electrodes.

A yellow-brown dispersion was created by ultrasonically preparing 1 mg mL^{-1} GO aqueous solution for 60 minutes. To create the GO/CPE, by casting the CPE surface with 10 µL of GO suspension and allowing it to be air-dried.

The electrochemically reduced GO (rGO) modified CPE (rGO/CPE) was synthesized by repeatedly scanning a CV (10 cycles) from 0 to -1.5 V at a scan rate of 50 mV s^{-1}.

For the PdNPs modified rGO/CPE (rGO-

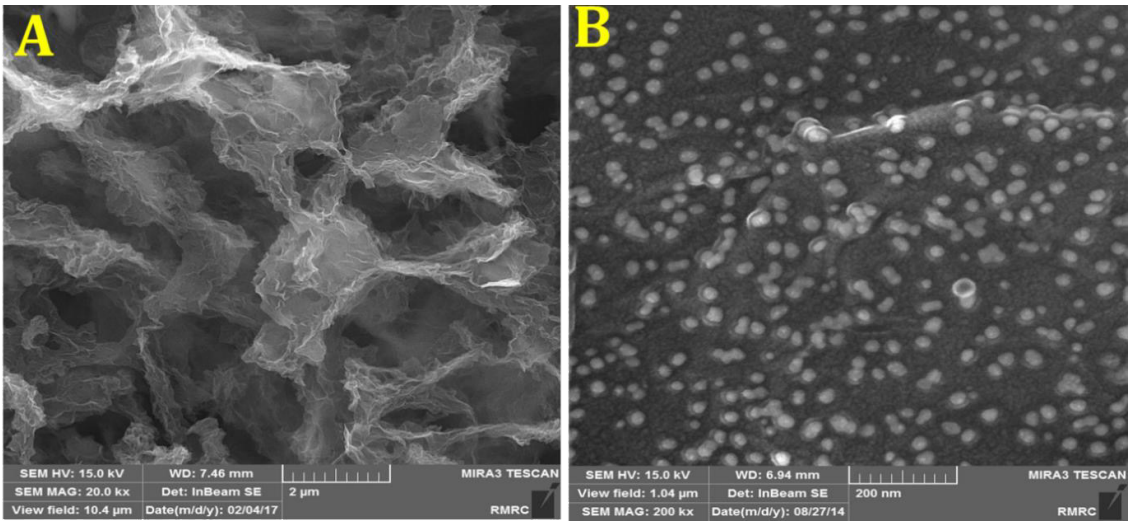

Fig. 1: SEM images of (A) Pd/CPE and (B) rGO-Pd/CPE.

Pd/CPE), the electrochemical codeposition was performed in a dearated PBS solution containing 1mM $PdCl_2$. The electrochemical deposition of PdNPs modified CPE (Pd/CPE) was accomplished in a dearated PBS containing 1mM $PdCl_2$.

RESULTS AND DISCUSSION

SEM image

Fig. 1 illustrates the surface morphology of the rGO-Pd and Pd on the CPE. As shown in Fig. 1A, rGO serves as a scaffold wrinkled sheet, anchoring the nucleation and loading of PdNPs, and preventing their aggregation. Conversely, PdNPs tends to accumulate on bare CPE, as depicted in Fig.1B. Compared to the plain CPE, PdNPs generate a structure on rGO that is relatively homogeneous, highly distributed, and of high density.

Electrochemical characterization of different modified electrode

Fig. 2 displays the CVs of electrochemical reduction of several customized electrodes in a phosphate buffer solution (pH=4) at a scan rate of 50 mV s^{-1}. The electrochemical reduction of GO on CPE is depicted in Fig. 2a. The appearance of a substantial cathodic peak current at approximately -1.2 V demonstrates the rapid and irreversible electrochemical reduction of oxygen-containing groups on GO [24-26]. In each subsequent cycle, the reduction peak significantly diminishes until it vanishes entirely in the fifth cycle [26-30]. As shown in Figs. 2b and 2c, $PdCl_2$ undergoes electrochemical reduction, and GO and $PdCl_2$ are simultaneously deposited on CPE. Fig. 2c displays clearly a distinct CV compared to that in Figs. 2b and 2a. Although the cathodic peak at -1.2 V persists due to the GO reduction, the reductive currents are noticeably greater than those in either the GO or Pd reduction, indicating the co-reduction of the GO and Pd. The reductive currents that show a decrease in Pd are also present in subsequent cycles, especially after the fifth cycle.

The electrochemical properties of the unmodified and modified electrodes were examined in a 5 mM solution of $K_3Fe(CN)_6$,. Since the surface chemistry of carbon-based electrodes is sensitive to the redox probe $Fe(CN)_6^{3-/4-}$ [31], it was utilized to assess the graphene electrode's ability to transfer charges.

The CVs of both unmodified and modified electrodes in a solution containing 5mM $K_3Fe(CN)_6$ and 0.1 M KCl are shown in Fig. 3. The results indicate that the rGO-modified CPE exhibited a significantly lower peak potential separation and a higher peak current compared to the unmodified CPE. This suggests that the reactive edge defects on graphene and the increased electroactive surface area of electrode 20 treated with rGO led to an accelerated electron transport [32, 33]. In addition, the improved current of rGO-Pd/CPE, compared to rGO/CPE, serves as evidence of PdNPs' function in facilitating electron transport

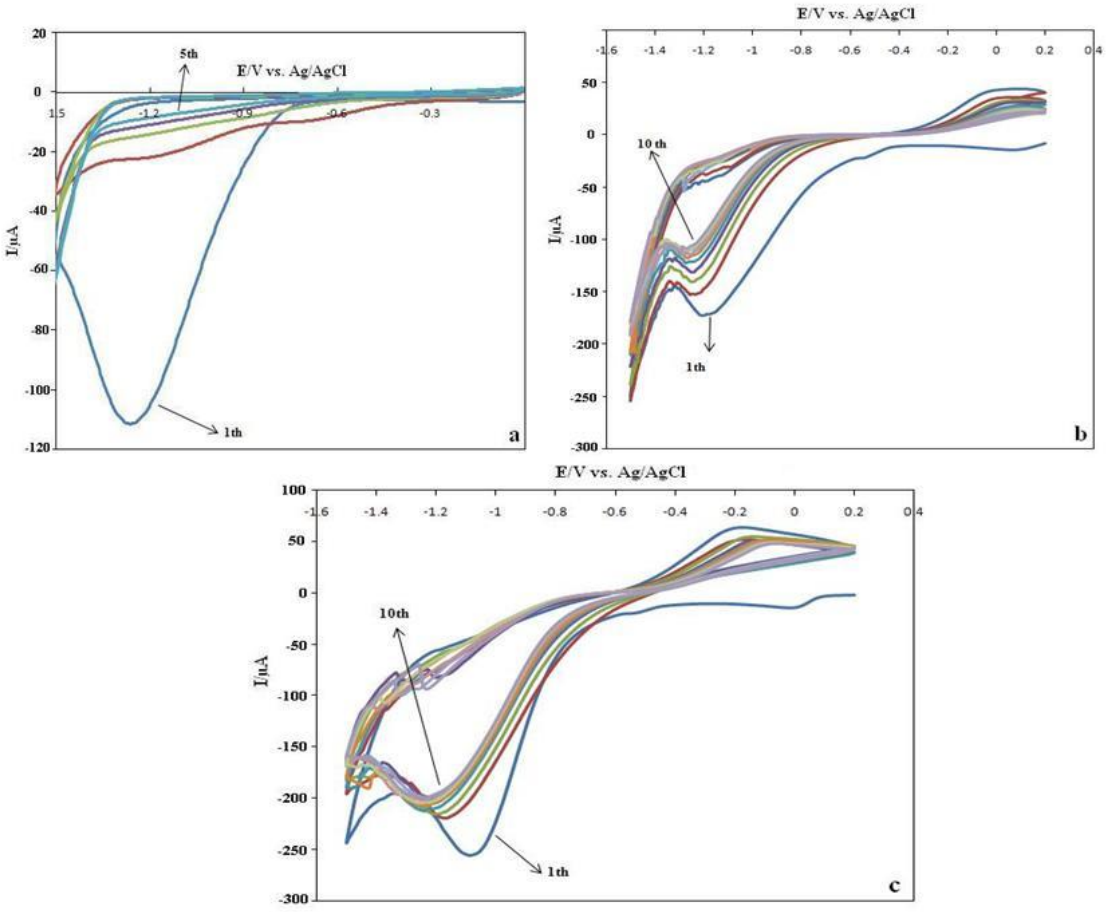

Fig. 2: CVs of electrochemical reduction of a) GO, b) Pd and c) co-deposition of GO and Pd in PBS (pH=4) at a scan rate of 50 mVS^{-1}.

and boosting the electroactive surface area. The high-density loading of PdNPs resulted from the electrochemical co-reduction of Pd and GO.

Effect of the thickness of the graphene-Pd nanocomposite film

One of the most important controlling factors in the experiment was the thickness of the graphene and Pd nanocomposite layer. Both GO and $PdCl_2$ were reduced during the cathodic sweep of CV. In Fig. 4 illustrates a link between the proton reduction current at -0.6 V and the number of cycles (N). As demonstrated, a significant increase in the proton reduction current was observed by increasing N up to 10. However, as the loading amount of deposits was increased further, the current began to decline, indicating that the nanocomposite film had become thick and the electron transfer rate had decreased. As a result, ten cycles were deemed to be the optimal number of prospective cycles for the remaining experiments.

Real surface area determination

It is crucial to understand the actual surface area of the electrode, which typically surpasses the geometric area, while studying solid electrodes and electrocatalysis. To this end, Trasatti and Petrii [34] go into great length regarding the methods for ascertaining the actual surface area. In the present investigation, the charges of the oxide reduction peaks are a viable measure to determine the actual surface area [35]. Based on the following equation, the actual surface area of the electrodes enhanced with nanoparticles was determined:

$S=Q_0/q_0$

Where Q_0 is the surface charge that can be calculated from the region under the oxygen desorption CV trace, and q_0 represents the charge necessary for the desorption of an oxygen

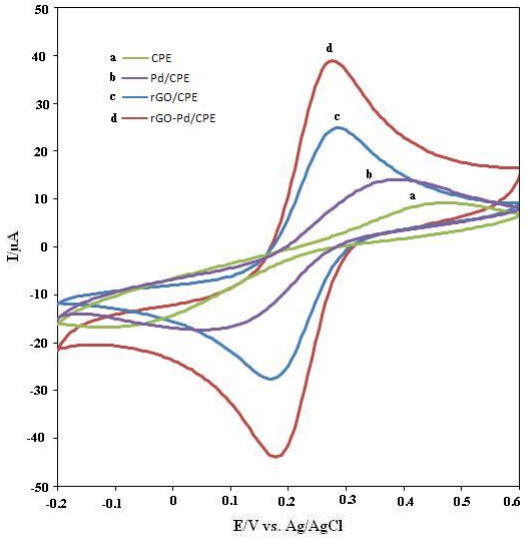

Fig. 3: CVs of bare and modified CPEs at 5mM $K_3Fe(CN)_6$ and 0.1 M KCl.

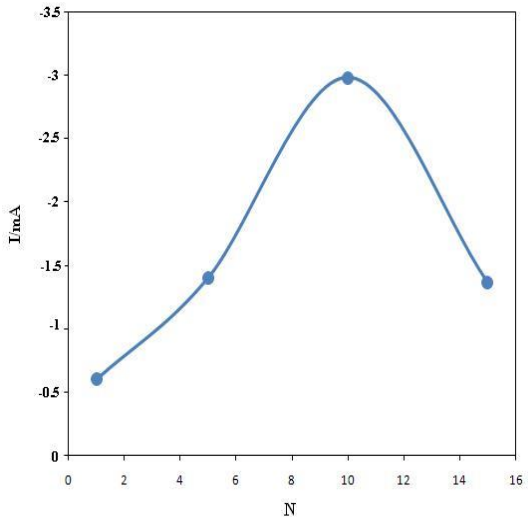

Fig. 4: Proton reduction current of rGO-Pd/CPE at -0.6 V as a function of N in 0.5 M H_2SO_4 solution and scan rate of 50 mV S^{-1}.

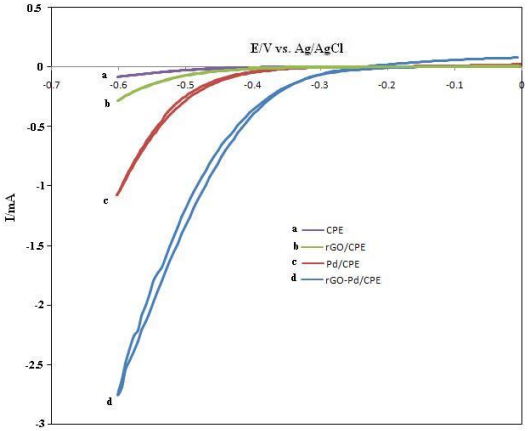

Fig. 5: Comparative CVs of (a) bare (CPE), (b) rGO/CPE (c) Pd/CPE and (d) rGO-Pd/CPE in 0.5 M H_2SO_4 and Scan rate of 50 mV s^{-1}.

monolayer on a smooth Au or Pd surface. The value of q_0 for the smooth Pd electrode is 424 cm^{-2} [36].

The actual surface area (S) for the Pd/CPE and rGO-Pd/CPE were calculated to be 0.07 cm^2 and 0.25 cm^2, respectively. Based on the findings, the high specific surface area of rGO significantly contributed to the effective surface area of rGO-Pd/CPE, which is 3.6 times more than that of Pd/CPE.

Electrocatalytic activity of the different modified electrodes for HER

Fig. 5 illustrates the comparative CVs of various electrodes in 0.5 M H_2SO_4 for HER. It can be seen that all of the modified electrodes exhibit electrocatalytic activity for HER when compared to bare electrodes. The reduction potentials of hydrogen generation were reduced to lower potentials than those of rGO/CPE. Moreover, both Pd/CPE and rGO-Pd/CPE exhibited strong current at the same potential. The findings indicate that the maximum electrocatalytic activity for HER is shown by rGO-Pd/CPE among the various electrodes. Thus, the electrochemical activity for HER can be significantly increased by adding Pd to rGO. Table 1 shows the potential of individual electrodes measured at a current value of -0.5 mA ($E_{-0.5}$), as well as the magnitude of the current

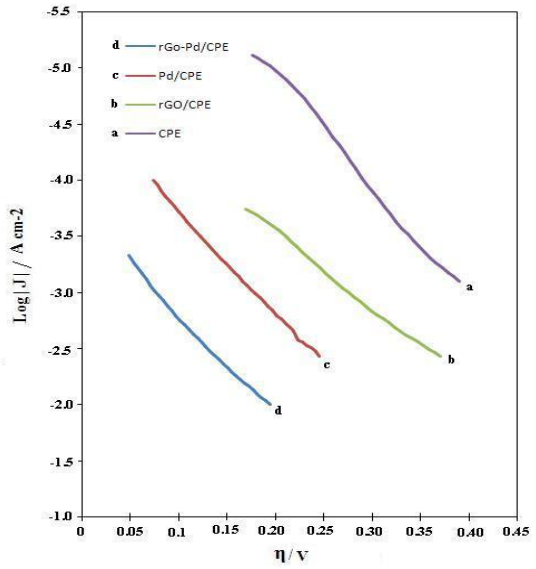

Fig. 6: Tafel plots for HER at (a) bare (CPE), (b) rGO/CPE (c) Pd/CPE and (d) rGO-Pd/CPE in 0.5 M H_2SO_4.

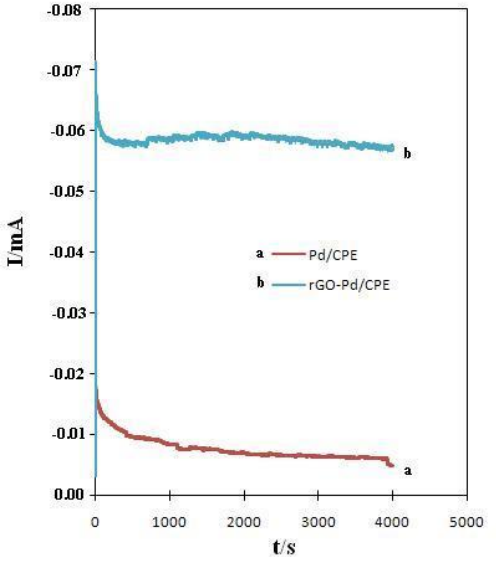

Fig. 7: CA curve at -0.3 V for the HER on (a) Pd/CPE and (b) rGO-Pd/CPE in 0.5 M H_2SO_4.

Table 1. Analysis of the CV responses of the bare and modified electrodes in 0.5M H_2SO_4 toward HER.

	$(I_m/I_b)^a$	$E_{-0.5}$(mV) at i=-0.5	$\Delta E_{-0.5}$(mV)
CPE	-	-780	-
CPE-rGo	2.1	-696	83
CPE-Pd	8.1	-540	240
CPE-rGo-Pd	20.1	-417	363

a: ratio of proton reduction current of modified to bare electrode at switching potential (E=-0.6 mV).

ratio of modified to naked electrodes at switching potential (E=-0.6 mV). The data presented in this table demonstrate that the values of $E_{-0.5}$ significantly drop from bare to modified electrodes. Notably, the hybrid catalyst has the lowest overpotential in comparison to other electrodes, suggesting better electrocatalytic activity for HER. At -0.6 mV, the I_m/I_b values for CPE-rGo, CPE-Pd, and CPE-rGoPd were approximately 2, 8, and 20 times greater than those for the bare electrode, respectively. Additionally, as shown in Fig. 5, it is obvious that the onset potential of HER at rGo-Pd is higher than that of the other electrodes, indicating its superior electrocatalytic activity towards HER.

Kinetic parameters and mechanism

To assess the electrocatalytic activities of the electrodes, steady-state polarization curves of the HER at bare and modified electrodes were determined. The related Tafel plots (log J vs. η) can be seen in Fig. 6. A scan rate of 2 mV s^{-1} was used to record the polarization curves in 0.5 M H_2SO_4.

As is shown in Fig. 6, the curves follow a typical Tafel behavior based on the following equation:

$$logJ = logJ_0 - \frac{\alpha F}{2.3RT}\eta$$

where b is the Tafel slope, $\eta\eta$ is the overpotential, and J is the steady-state current density and Jo is the exchange current density. Tafel plot extrapolation to the intercept yields log. The graph's slopes can be used to determine the Jo and Tafel slope.

As can be seen, rGO-Pd/CPE increased electrocatalytic activity in the following order: Pd/CPE>rGO/CPE>CPE. This demonstrates an excellent agreement between the findings of both investigations and CV experiments. Further, the rGO-Pd/CPE has the strongest electrocatalytic impact for HER.

Table 2. Kinetic parameters for HER at bare and modified electrodes

Electrode	$-\log\lvert J_0\rvert$ (A cm^{-2})	b (mV dec^{-1})	α
CPE	7.1	97	0.6
rGO/CPE	4.9	146	0.40
Pd/CPE	4.6	110	0.53
rGO-Pd/CPE	3.6	112	0.53

Table 2 lists the Tafel parameters for HER on unmodified and modified CPEs. As can be seen, the rGO-Pd/CPE electrode exhibits stronger catalytic efficacy towards HER than the other modified electrodes, despite having a significantly higher J_o (0.25×10^{-3} mA cm^{-2}).

The HER in acidic media has three potential reaction stages, as reported by study [37]. The rate-limiting step, also known as rate determining step or rds, determines the Tafel slope, which is an inherent feature of a catalyst.

To elucidate the basic procedures, it is necessary to determine and interpret the Tafel slope. For multi-step reactions, the value of the charge-transfer coefficient depends on the rds [38]. According to the general model for the HER mechanism, when the value of α is 0.5 and the Tafel slope shifts to 120 mV dec^{-1}, the Volmer reaction controls the HER. In this case, the α is approximately 0.5 on the modified electrodes and their Tafel slopes are near 120 mv dec^{-1} (see Table 2). Therefore, it can be concluded that the Volmer step must regulate the HER on the modified electrodes.

Stability and renewability studies

The stability of rGO-Pd/CPE and Pd/CPE was assessed by using CA and CV techniques. To explore their stability, 100 repetitive CV cycles of the rGO-Pd/CPE and Pd/CPE were recorded by repeatedly scanning in a solution of 0.5 M H_2SO_4 from 0.0 to -0.5 V at a scan rate of 50 mV s^{-1}. The results demonstrate that, as opposed to Pd/CPE, rGO-Pd/CPE significantly reduces the electrocatalytic current of HER at switching potential. Specifically, after 50 cycles, the current diminished by up to 6% and 51%, and after 100 cycles up to 18% and 68% of the initial current value for rGO-Pd/CPE and Pd/CPE. This indicates that the graphene-Pd hybrid has good stability towards HER. It should be noted, however, that variations in voltamogarm resulting from subsequent cycles are not implausible [39].

CONCLUSION

A one-step, facile, and rapid electrochemical method was used in the co-deposition of GO and PdNPs onto CPE. The resulting rGO-Pd/CPE was characterized using SEM, CV and CC techniques. PdNPs exhibited a fairly homogenous and high dispersed structure with high density on the rGO compared to the bare CPE. The rGO-Pd/CPE showed superior electrocatalytic activity toward HER compared to other electrodes. The kinetic parameters, including transfer coefficient and exchange current density, as well as the HER mechanism were determined from the Tafel plot. Furthermore, the rGO-Pd/CPE was renewable and demonstrated good stability for HER.

ACKNOWLEDGMENT

The authors express their gratitude to Shiraz University Research Council for the support of this work.

CONFLICT OF INTEREST

The authors declare no conflicts of interest.

REFERENCES

1. Mao X, Qin Z, Ge S, Rong C, Zhang B, Xuan F-Z. Strain engineering of electrocatalysts for hydrogen evolution reaction. Materials horizons. 2022;10. https://doi.org/10.1039/d2mh01171a
2. Veeramani K, Janani G, Kim J, Surendran S, Lim J, Jesudass SC, et al. Hydrogen and value-added products yield from hybrid water electrolysis: A critical review on recent developments. Renewable and Sustainable Energy Reviews. 2023;177:113227. https://doi.org/10.1016/j.rser.2023.113227
3. Walter MG, Warren EL, McKone JR, Boettcher SW, Mi Q, Santori EA, et al. Solar Water Splitting Cells. Chemical Reviews. 2010;110(11):6446-73. https://doi.org/10.1021/cr1002326
4. Liu Y, Wang Q, Zhang J, Ding J, Cheng Y, Wang T, et al. Recent Advances in Carbon-Supported Noble-Metal Electrocatalysts for Hydrogen Evolution Reaction: Syntheses, Structures, and Properties. Advanced Energy Materials. 2022;12(28):2200928. https://doi.org/10.1002/aenm.202200928
5. Zhang W, Xi R, Li Y, Zhang Y, Wang P, Hu D. Recent development of transition metal doped carbon

materials derived from biomass for hydrogen evolution reaction. International Journal of Hydrogen Energy. 2022;47(76):32436-54. https://doi.org/10.1016/j.ijhydene.2022.07.167
6. Abdelghafar F, Xu X, Jiang SP, Shao Z. Designing single-atom catalysts toward improved alkaline hydrogen evolution reaction. Materials Reports: Energy. 2022;2(3):100144. https://doi.org/10.1016/j.matre.2022.100144
7. Liu Z, He T, Jiang Q, Wang W, Tang J. A review of heteroatomic doped two-dimensional materials as electrocatalysts for hydrogen evolution reaction. International Journal of Hydrogen Energy. 2022;47(69):29698-729. https://doi.org/10.1016/j.ijhydene.2022.06.306
8. Wang H-F, Tang C, Zhao C-X, Huang J-Q, Zhang Q. Emerging Graphene Derivatives and Analogues for Efficient Energy Electrocatalysis. Advanced Functional Materials. 2022;32(42):2204755. https://doi.org/10.1002/adfm.202204755
9. Lao M, Li P, Jiang Y, Pan H, Dou S, Sun W. From Fundamentals and Theories to Heterostructured Electrocatalyst Design: An In-depth Understanding of Alkaline Hydrogen Evolution Reaction. Nano Energy. 2022;98:107231. https://doi.org/10.1016/j.nanoen.2022.107231
10. Ding J, Yang H, Zhang S, Liu Q, Cao H, Luo J, et al. Advances in the Electrocatalytic Hydrogen Evolution Reaction by Metal Nanoclusters-based Materials. Small. 2022;18. https://doi.org/10.1002/smll.202204524
11. Mehrgardi M, Khoshfetrat SM. Amplified Electrochemical Genotyping of Single-Nucleotide Polymorphisms using Graphene-Gold Nanoparticles Modified Glassy Carbon Platform. RSC Advances. 2015. https://doi.org/10.1039/C5RA03794H
12. Zhou G, Yin L, Ren W, Li F, Cheng H-M. Graphene/metal oxide composite electrode materials for energy storage. Nano Energy. 2012;1:107–31. https://doi.org/10.1016/j.nanoen.2011.11.001
13. Singh A, Das C, Indra A. Scope and prospect of transition metal-based cocatalysts for visible light-driven photocatalytic hydrogen evolution with graphitic carbon nitride. Coordination Chemistry Reviews. 2022;465. https://doi.org/10.1016/j.ccr.2022.214516
14. Xiong L, Qiu Y, Peng X, Liu Z, Chu P. Electronic structural engineering of transition metal-based electrocatalysts for the hydrogen evolution reaction. Nano Energy. 2022;104:107882. https://doi.org/10.1016/j.nanoen.2022.107882
15. Normohammadi S, Bahmani F, Fotouhi L, Khoshfetrat SM. Electrodeposited nickel nanocone/NiMoO4 nanocomposite designed as superior electrode materials for high performance supercapacitor. International Journal of Hydrogen Energy. 2021;47. https://doi.org/10.1016/j.ijhydene.2021.11.161
16. Claussen J, Franklin A, Haque A, Porterfield D, Fisher T. Electrochemical Biosensor of Nanocube-Augmented Carbon Nanotube Networks. ACS nano. 2009;3:37-44. https://doi.org/10.1021/nn800682m
17. Meng H, Wang C, Shen P, Wu G. Palladium thorn clusters as catalysts for electrooxidation of formic acid. Energy Environ Sci. 2011;4:1522-6. https://doi.org/10.1039/C0EE00702A
18. Sadeghian Renani T, Khoshfetrat SM, Arjomandi J, Shi H, Khazalpour S. Fabrication and Design of New Redox Active Azure A/3D Graphene Aerogel and Conductive Trypan Blue–Nickel MOF Nanosheet Array Electrodes for an Asymmetric Supercapattery. Journal of Materials Chemistry A. 2021;9. https://doi.org/10.1039/D1TA02850B
19. Ren P-G, Yan D-X, Ji X, Chen T, Zhong G. Temperature dependence of graphene oxide reduced by hydrazine hydrate. Nanotechnology. 2011;22:055705. https://doi.org/10.1088/0957-4484/22/5/055705
20. Feng M, Feng H. Effect of Reducing Agent on the Chemical Reduction of Graphene Oxides. Journal of nanoscience and nanotechnology. 2013;13:937-41. https://doi.org/10.1166/jnn.2013.6005
21. Pham VH, Pham HD, Dang TT, Hur SH, Kim EJ, Kong BS, et al. Chemical reduction of an aqueous suspension of graphene oxide by nascent hydrogen. Journal of Materials Chemistry. 2012;22(21):10530-6. https://doi.org/10.1039/C2JM30562C
22. Chen W, Yan L, Bangal P. Chemical Reduction of Graphene Oxide to Graphene by Sulfur-Containing Compounds. Journal of Physical Chemistry C. 2010;114:19885-90. https://doi.org/10.1021/jp107131v
23. Moon I, Junghyun L, Ruoff R, Lee H. Reduced graphene oxide by chemical graphitization. Nature communications. 2010;1:73. https://doi.org/10.1038/ncomms1067
24. Shan W, Ting, Prakash P, Chen S-M, Ramiah S. Direct Electrochemistry of Catalase Immobilized at Electrochemically Reduced Graphene Oxide Modified Electrode for Amperometric H_2O_2 Biosensor. International Journal of Electrochemical Science. 2011;6.
25. Deng K-Q, Zhou J-h, Li X-F. Direct electrochemical reduction of graphene oxide and its application to determination of l-tryptophan and l-tyrosine. Colloids and Surfaces B: Biointerfaces. 2013;101:183-8. https://doi.org/10.1016/j.colsurfb.2012.06.007
26. Chen L, Tang Y, Wang K, Liu C, Luo S. Direct electrodeposition of reduced graphene oxide on glassy carbon electrode and its electrochemical application. Electrochemistry Communications - ELECTROCHEM COMMUN. 2011;13:133-7. https://doi.org/10.1016/j.elecom.2010.11.033
27. Mani V, Devadas D-B, Chen S-M. Direct electrochemistry of glucose oxidase at electrochemically reduced graphene oxide-multiwalled carbon nanotubes hybrid material modified electrode for glucose biosensor. Biosensors and Bioelectronics. 2012. https://doi.org/10.1016/j.bios.2012.08.045
28. Chen T-W, Sheng Z-H, Wang K, Wang F-B, Xia X-H. Determination of Explosives Using Electrochemically Reduced Graphene. Chemistry, an Asian journal. 2011;6:1210-6. https://doi.org/10.1002/asia.201000836
29. Wang Z, Zhou X, Zhang J, Boey F, Zhang H. Direct Electrochemical Reduction of Single-Layer Graphene Oxide and Subsequent Functionalization with Glucose Oxidase. The Journal of Physical Chemistry C. 2009;113. https://doi.org/10.1021/jp906348x
30. Ping J, Wang Y, Fan K, Wu J, Ying Y. Direct electrochemical reduction of graphene oxide on ionic liquid doped screen-printed electrode and its electrochemical biosensing application. Biosensors & bioelectronics. 2011;28:204-9. https://doi.org/10.1016/j.bios.2011.07.018
31. Chen P, Fryling M, McCreery R. Electron Transfer Kinetics at Modified Carbon Electrode Surfaces: The Role of Specific Surface Sites. Analytical Chemistry - ANAL CHEM. 1995;67. https://doi.org/10.1021/ac00114a004

32. Brownson D, Banks C. Graphene Electrochemistry: An Overview of Potential Applications. The Analyst. 2010;135:2768-78. https://doi.org/10.1039/c0an00590h
33. Kampouris D, Banks C. Exploring the physicoelectrochemical properties of graphene. Chemical communications (Cambridge, England). 2010;46:8986-8. https://doi.org/10.1039/c0cc02860f
34. Trasatti S, Petrii OA. Real surface area measurement in electrochemistry. Journal of Electroanalytical Chemistry. 1991;63:353-76. https://doi.org/10.1016/0022-0728(92)80162-W
35. Łukaszewski M, Czerwiński A. Electrochemical preparation and characterization of thin deposits of Pd-noble metal alloys. Thin Solid Films. 2010;518:3680-9. https://doi.org/10.1016/j.tsf.2009.10.008
36. Woods R, Bard A. Electroanalytical chemistry. Marcel Dekker: New York; 1976.
37. Conway BE, Tilak BV. Interfacial processes involving electrocatalytic evolution and oxidation of H2, and the role of chemisorbed H. Electrochimica Acta. 2002;47(22):3571-94. https://doi.org/10.1016/S0013-4686(02)00329-8
38. Łoś P, Rami A, Lasia A. Hydrogen Evolution Reaction on Ni-Al Electrodes. Journal of Applied Electrochemistry. 2002;23:135-40. https://doi.org/10.1007/BF00246950
39. Kissinger P, Heineman WR. Laboratory Techniques in Electroanalytical Chemistry, revised and expanded: CRC press; 2018.